ORIGINAL ARTICLE

Stormwater management of biochar-amended green roofs: peak flow and hydraulic parameters using combined experimental and numerical investigation

Shan Huang [1,2,3] · Disheng Huang [1,2,3] · Ankit Garg [1,2,3] · Mingjie Jiang [1,2,3] · Guoxiong Mei [1,2,3] · Sreeja Pekkat [4]

Abstract

Green roofs have been suggested as one solution to manage stormwater in cities. Soil amendments such as biochar appear to be very promising owing to its water retention capacity. Furthermore, biochar is more stable with time (expected half-life over 100 years) than other biomass (fibers), which is likely to degrade at higher rate upon microbial action. Rational utilization of biochar-amended soil in substrates is the critical factor for improving ability of stormwater management (peak-flow reduction and delay). The objective of this study is to evaluate the hydraulic performance of green roofs amended with biochar. Laboratory experiments combined with numerical approach were adopted to achieve the objective. A dual-layer substrate mode with biochar-amended soil was proposed for optimizing the ability of stormwater management. Four experimental columns were built to observe the hydraulic processes under artificial rainfall. Unsaturated hydraulic parameters of substrates were estimated by the inverse solution method. Numerical simulations have been conducted to explore the stormwater management of dual-layer substrates with biochar. Both biochar and vegetation are found to enhance saturated water content. However, their effects on hydraulic properties of soil were opposite, with vegetation having positive influence. Different biochar application modes showed varied performance in peak-outflow delay and reduction. In the selected rainstorm case, the substrate with 3 cm vegetated natural soil in upper layer and 12 cm biochar-amended soil showed a longer delay, higher reduction in peak outflow, and rainwater retention. The dual-layer substrate mode is a flexible utilization of biochar in green roofs. It provided a more reasonable design with the consideration of the local rainfall statistical data.

Keywords Green roof · Biochar · Substrate amendment · Stormwater management · Multilayer substrate

1 Introduction

Rapid urbanization is leading to faster reduction in natural infiltration surface area, which is further intensifying the urban-inundation disaster. The application of green roofs has increasing in China since the declaration of concept of Sponge City Construction (SCC) by the government of People's Republic of China at the end of 2014 [1]. The first group of 16 cities was selected as the pilot sponge cities (including Nanning, Guangxi province) in 2015, and 1 year later, the pilot program was expanded to another 14 cities. Green roof is one of the measures in SCC and developing fast in the recent years, as reports shown 1,500,000 m^2 green roof area in Beijing at 2011 and 1,450,000 m^2 in Shanghai at 2012 [2]. Some researches were conducted on the practical green roof in China to explore its hydraulic and thermal performance [3, 4]. The green roofs play a significant role in managing the

✉ Mingjie Jiang
20180121@gxu.edu.cn

✉ Guoxiong Mei
meiguox@163.com

1 College of Civil Engineering and Architecture, Guangxi University, Nanning 530004, People's Republic of China

2 Key Laboratory of Disaster Prevention and Structural Safety of Ministry of Education, Guangxi University, Nanning 530004, People's Republic of China

3 Guangxi Key Laboratory of Disaster Prevention and Structural Safety, Guangxi University, Nanning 530004, P. R. China

4 Department of Civil Engineering, Indian Institute of Technology Guwahati, Guwahati, India

rainwater by affecting the outflow quantity and quality. As roofs account for considerable areas in cities, the green roofs have become an effective way to alleviate stormwater.

Many studies suggested that biochar is one of the potential soil amendments. Biochar is one of the green materials that has attracted more attention in recent years for its application in green infrastructure (green roofs; bio-filters; green corridors [5–7]). It is a stable carbon charcoal produced from the pyrolysis of plant-based or poultry-based biomass. As a soil amendment, it has many advantages such as: (1) enhanced water retention capacity; (2) mitigating nutrient leaching; and (3) reducing the weight of the green roof [6, 7]. In agriculture, biochar also has benefits in improving soil fertility and thus enhances plant growth [8]. The characteristics of the biochar depend on the specific surface area, porosity, and the chemical composition, which may vary with the input feedstock type for pyrolysis and pyrolysis temperatures (300–700 °C) [9]. Furthermore, biochar has much higher stability and resistance to microbial degradation compared to other biomass. Half-life of biochar is expected to be in 100–1000 years [10]. In addition, aging of biochar is likely to enhance water sorption in coarse-textured soils as observed in recent studies [11–13]. Thus, even from a long-term perspective, biochar has a potential as a green roof amendment for stormwater management.

Studies have discussed biochar influences on the infiltration rate of the soil. The effect of biochar is not definite in many studies. Most of the results indicated that the biochar decreased the permeability of coarse-grained soil but showed no significant changes or slightly increased in the saturated hydraulic conductivity of fine material (i.e., clayey soil) [14–16]. However, according to the studies by Bordoloi et al. [17] and Gopal et al. [18], the biochar-amended soil has developed fewer and smaller cracks than natural soil after drying-wetting cycles and thus showed a lower infiltration rate in the natural environment [18]. The infiltration rate is one of the key parameters to the green roofs, which affects the ability of stormwater management. Most of the above studies were conducted on single layered soil and may not be directly applicable in interpretation of water flow in multi-layered soil (as found in green roofs; [19]) amended with biochar. Beck et al. [20] analyzed saturated water retention and runoff quality and quantity of green roof substrate with and without biochar amendment. Their study found that biochar improved water retention and runoff quality (i.e., decreased in discharge of total nitrogen, phosphate, and organic carbon). Chen et al. [21] found that presence of biochar (10–15%) enhanced water retention and reduced average temperature in green roofs substrate. Kuoppamäki, Lehvävirta [7] found that biochar effects may vary (positive or negative) depending on type of biochar and plant. Their studies cautioned that biochar applications cannot be generalized and require a more customized approach depending on substrate, plant, and climate conditions. Similarly, Olszewski and Eisenman [22] found that effects of

biochar may vary depending on type of plant. Their study found that biochar has better effects in peppermint than basil plant. As far as authors are aware, there is lack of systematic study on analyzing water flow (permeability, peak-outflow, storage capacity) in multi-layer substrate with biochar. Furthermore, there is lack any interpretation of unsaturated soil hydraulic parameters that is essential in seepage analysis. Such study may be useful in design of preliminary guidelines for Sponge City Construction (SCC) and Low Impact Development (LID) in Guangxi province of China, where experiences sub-tropical climate similar to those in Singapore, Malaysia, Brazil, Indonesia, and some parts of Asia.

The study aims to evaluate the hydraulic performance of green roofs with biochar and optimize its ability in stormwater management. To achieve these goals, four experimental columns containing local soil and native plant (*Zoysia matrella* grass species) were built to observe the hydraulic processes (e.g., surface ponding and bottom drainage) under artificial rainfall. Unsaturated hydraulic parameters of soils were derived in four columns by using inverse analysis. Numerical simulation was conducted to explore the mechanism of stormwater management performance of different biochar application modes in the green roof substrate.

2 Experiment and simulation

2.1 Substrate materials including in-house biochar preparation

In accordance with the policy of Sponge City Construction (SCC) and Low Impact Development (LID) in China, full use of local natural soil instead of the cultivated soil or the commercial substrate is promoted. The soil adopted in this study was collected from a natural slope in Nanning city, located in the southern part of China. For improving the uniformity of the soil in column, remolding soil (grinded and sieved through 2 mm) was done before the addition of the biochar and any compaction. The properties of the remolded soil are tabulated in Table 1. According to the Unified Soil Classification System (USCS, ASTM D2487), the tested soil can be classified as Lean clay (CL). Although, it is understood that clay is vulnerable to cracking, however, considering its abundance in South-west Guangxi province make it more feasible economically and in practice to be adopted for green infrastructure. Although, a systematic cost-benefit analysis [23] is required in terms of using such soil including any amendment in green infrastructure considering its engineering, environmental, and economic impact.

As shown in Fig. 1, the biochar was manufactured in-house by pyrolyzing cedar at 750 °C. A large number of grooves (pores) (refer to Fig. 1) implies enhanced specific surface area

Table 1 Basic properties of the soil and biochar

	Soil properties	Standard	Natural soil	Biochar (powder form)	Biochar-amended soil
Particle size distribution	Coarse sand (4.75–2) mm	ASTM D422	0%	0%	0%
	Medium sand (0.425–2) mm		0.5%	10.2%	1.4%
	Fine sand (0.075–0.425) mm		1.7%	56.6%	7.6%
	Silt (0.002–0.075) mm		44.7%	32.5%	87.9%
	Clay (< 0.002) mm		53.1%	0.7%	3.1%
Compaction properties	Optimum moisture content	ASTM D698	16.45%	-	19.7%
	Maximum dry density (g/cm^3)		1.80	-	1.60
Atterberg limits	Plastic limit (PL)	ASTM D4318	22.3%	-	22.7%
	Liquid limit (LL)		66.7%	-	51.0%
	Plastic index (PI)		44.4	-	28.3
In-situ dry density (g/cm^3)		ASTM D1556	1.55	-	-
Specific gravity		ASTM D854	2.71	-	-
Saturated hydraulic conductivity (mm/min)		ASTM D5084	0.36	-	0.22

and provided more porosity for retaining water. The biochar-amended soil was made by mixing the biochar powder (after passing 2 mm sieve) with soil in powder form as shown in Fig. 1. Amendment ratio of 1:10 by weight was adopted as it corresponds to maximum efficiency of biochar in retaining unsaturated water and crack suppression [17].

For setting the same baseline for the test materials, as well as the same load condition in the design of green roofs, all of the soil columns (as mentioned in next subsection) were compacted at a dry density of 1.2 g/cm^3. This value lies within the range specified by Emilsson and Rolf [24]. The degree of compaction (DOC) of natural soil columns (NS) and biochar-amended soil columns (BAS) was 67% and 75%,

respectively. It should be noted that this compaction degree was much lower than researches on landfill cover material (compacted usually at 90%); this is because substrate with high DOC may not provide the required healthy balance between water supply and gaseous exchange for ornamental plants in green roofs [25]. Vaseline was applied along the inner wall of the container to avoid the influence of friction and preferential flow between the wall and soil column [26]. Further studies are needed to identify the optimal value of compaction considering the growth of native vegetation and the influence of climatic conditions.

The two vegetated columns, vegetated natural soil column (VNS) and vegetated biochar-amended soil column (VBAS),

Fig. 1 Apparent feature and microscopic property of biochar
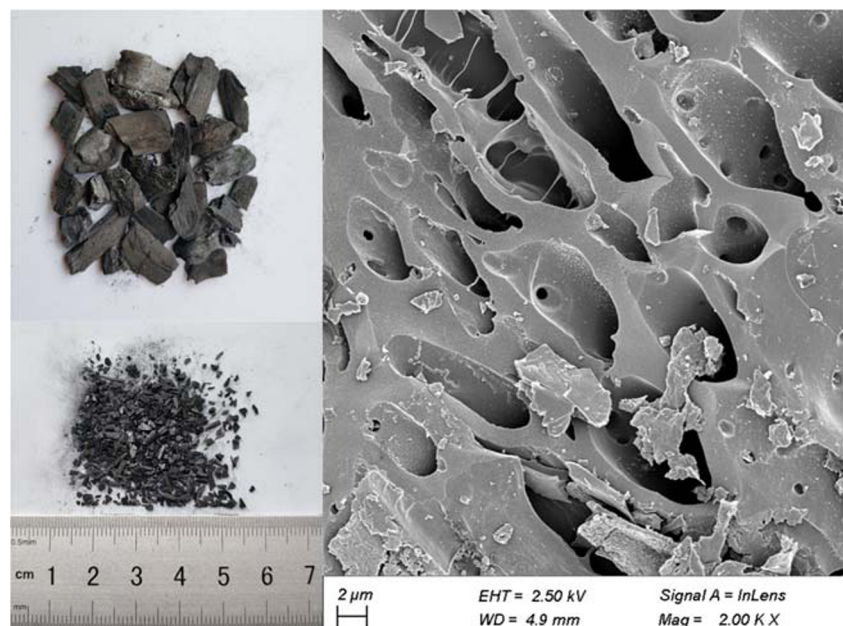
were fabricated through an identical procedure as bare soil columns. The commercial grass turf (*Zoysia matrella*) adopted in this study is a perennial grass. It is popularly used as the lawn grass in the southern part of China. It has the advantages of drought-resistant and barren tolerance [27]. The commercial turf was previously grown for eight months in a nursery. The vegetated soil columns were irrigated regularly for 1 month (30 days) before the rainfall infiltration test. The details of the four soil columns are tabulated in Table 2.

2.2 Design and development of apparatus

The laboratory infiltration test is one of the effective ways to understand the hydraulic process of green roof substrates [28, 29]. In this study, soil columns (15 cm in height and 30 cm in diameter, refer to Fig. 2) are designed and built for simulating one-dimensional infiltration process in extensive green roofs [30]. Surface ponding was allowed to monitor the saturated infiltration rate during the rain [31]. There were five drain holes and a thin filter plate under the soil column containers to allow free drainage in the bottom boundary of soil samples. As shown in Fig. 2, the artificial rainfall was simulated by using a rainfall system, including a water-replenished Mariotte bottle and a porous disk, which has been proved to be effective in constant-intensity rainfall simulation [32]. The rainfall simulator was fixed at the upper edge of the soil column container to maintain a constant raindrop height (10 cm) during the rainfall process.

A 5-h rainfall with a steady intensity of 0.4 mm/min was applied to simulate a short-term rainstorm. This intensity is equal to a 5-year return period rainstorm intensity [33, 34] in Nanning city. The moisture sensors (EC-5; METER Devices, refer to Fig. 2) were located at 5 cm and 10 cm depths below the surface of soil columns. Monitoring of moisture changes at these depths can provide a clear idea of water flow and storage within the green roof substrate [19]. Readings of volumetric water content (VWC), ponding variation, and the drainage were obtained simultaneously at 3-min interval during the rain. Based on the pan evaporation rate (i.e., 2.6–3.2 mm/day) measured during the test, the amount of evaporation can be assumed to be insignificant in shorter duration of test [35].

Fig. 2 Test set-up and sensors

Although soil column experiments have been widely used to study the hydraulic characteristics of green roofs, it still has some deficiency. One of the limitations is the vertical preferential flow along the gap between barrel wall and soil column. The influence can be reduced by smearing Vaseline on the barrel walls and increasing the diameter of soil columns. The size of the present experimental pot was 30 cm in diameter, which lies within range of previous studies such as Ni et al. [36] (i.e., 20 cm), Quinn, Dussaillant [29] (i.e., 14 cm), and Leung et al. [37] (i.e., 30 cm). Another limitation is that the rainfall simulators used in this study cannot simulate the varying rainfall intensity as the actual rainfall events. Therefore, this study adopts the method of Yang et al. [4], and further analyzes the runoff quantity of green roof under the actual rainfall through numerical simulation.

2.3 Simulation

The numerical program, HYDRUS-1D, version 4.16 [38], was used to simulate the hydraulic behavior of the substrates in the green roof [39]. The one-dimensional uniform water

Table 2 Details of the experimental soil columns

Columns	Substrate material	Vegetation	Dry density ρ_d/g · cm^{-3}	Initial water content (rain beginning) θ/m^3 · m^{-3}	
				z = 5 cm	z = 10 cm
NS	Natural soil	-	1.20	0.32	0.33
VNS	Natural soil	Grass		0.39	0.37
BAS	Soil-biochar mix	-		0.27	0.29
VBAS	Soil-biochar mix	Grass		0.37	0.35

movement was simulated by solving the modified form of the Richards' equation:

$$\frac{\partial \theta}{\partial t} = \frac{\partial}{\partial x}\left[K\left(\frac{\partial h}{\partial x} + \cos\alpha\right)\right] - S$$

The finite-difference method (FDM) was used for discretization of the Richards' equation. The soil hydraulic prosperity is usually given using the van Genuchten-Mualem (VGM) model:

$$S_e = \frac{\theta - \theta_r}{\theta_s - \theta_r} = \begin{cases} \dfrac{1}{(1 + |\alpha h|^n)^m} & h < 0 \\ 1 & h > 0 \end{cases}$$

$$K(S_e) = k_s S_e^{\,l}\left(1 - \left[1 - S_e^{1/m}\right]^m\right)^2$$

The unsaturated hydraulic parameters, including residual water content (θ_r) and saturated water content (θ_s), model-shape parameters α, n, and m ($m = 1 - 1/n$), the pore-connectivity parameter l, and saturated hydraulic conductivity k_s, were estimated by using the inverse method. The inverse procedure in HYDRUS-1D combines the Levenberg-Marquardt non-linear parameter optimization method [40] with a numerical solution of the Richards' equation.

In this study, soil, boundary and domain (size of 15 cm of column) conditions similar to four soil columns (as mentioned in previous section) were built in HYDRUS-1D. An atmospheric boundary condition with precipitation was imposed on the upper surface. A free drainage boundary condition was applied at the bottom. For the estimation of hydraulic parameters, measured water content before the rainfall was set as the initial condition. The measured hydrological processes data (i.e., ponding and drainage) and water contents during rainfall were inputted for the estimation.

According to the existing research [41], the residual water content θ_r and the pore-connectivity parameter l in the model were least sensitive to the bottom drainage and the water content. Residual water content and pore-connectivity parameter were fixed respectively as 0.01 and 0.5 as suggested by Mualem [42]. The saturated hydraulic conductivity of bare soil columns (refer to Table 1) was set to the measured values. In total, 4 parameters of the VGM model, including saturated moisture content θ_s, saturated hydraulic conductivity k_s (only estimated in VNS and VBAS), and two shape parameters α and n, were estimated based on methods similar to previous works [31]. The goodness of the estimation can be reflected by the R^2 value for regression of the observed values versus fitted values. R^2 value of 1 indicates a perfect correlation between the fitted and observed data.

3 Result and discussion

3.1 Experimental result

During the rain simulation experiment, column BAS generated a visible surface ponding (refer to Fig. 3) at the 90th min from the start of the rain. Ponding was found to increase at a steady rate of 0.1 mm/min. The ponding phenomenon was not observed in the other three soil columns, which indicated that column BAS possessed a lowest infiltration rate than the other soil columns. The surface water level progressively reached to a maximum height of 20 mm at the end of the rain. The ponding water permeated into the soil column with a steady infiltration rate of 0.2 mm/min and dissipated at approximately, 400th min.

Figure 4 compares the drainage (drainage volume divided by the cross-sectional area of the soil column) among soil columns. Drainage was generated progressively from these four tested soil columns. As shown in Fig. 4, column VNS generated drainage at the 16th min, followed by NS and VBAS. BAS shows the latest in drainage occurrence with a 182 min delay after the rain beginning.

The drainage from the four soil columns increased linearly after the occurrence, which indicated a steady infiltration rate in the soil. As shown in Fig. 5, the drainage rate of column NS, VNS, and VBAS stabilized at 0.4 mm/min, which is close to the rainfall intensity. In comparison, BAS showed a slower drainage rate, with the velocity at about 0.2 mm/min. The steady drainage rate of BAS was approximately equal to the saturated hydraulic conductivity (represented by the dotted lines in Fig. 5). The rainfall intensity exceeded the saturated infiltration rate of BAS, and thus caused a part of the rainwater to accumulate on the surface of the soil column. However, the drainage rates of NS, VNS, and VBAS were close to the
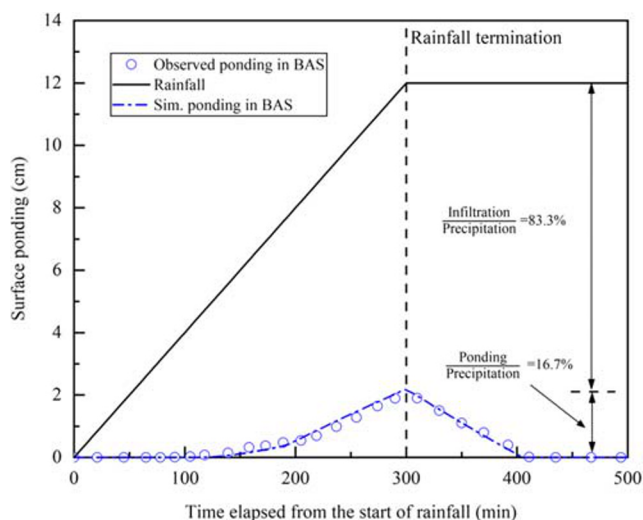

Fig. 3 The measured results and simulation curve of surface ponding above column BAS
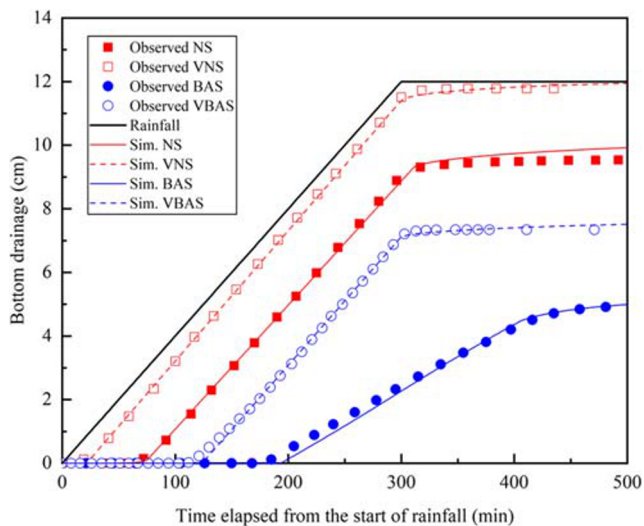
Fig. 4 The measured results and simulated curve of bottom drainage

rainfall intensity, because of their higher saturated hydraulic conductivities compared to rainfall intensity.

3.2 Unsaturated hydraulic parameters of treated and untreated soil

The optimized unsaturated hydraulic parameters of the four soil columns are summarized in Table 3. Figures 3 and 4 show the measured data (in color marks) and calculated results (in lines). The high agreement between the measured data and simulation results, as well as the R^2 value (refer to Table 3), indicated that the numerical simulations were able to capture the bottom drainage and surface ponding of these four soil columns. The optimized parameters were able to reflect the hydraulic characteristics of these substrate materials.

As shown in Table 3, the saturated water content of biochar-amended soil columns (BAS and VBAS) was higher
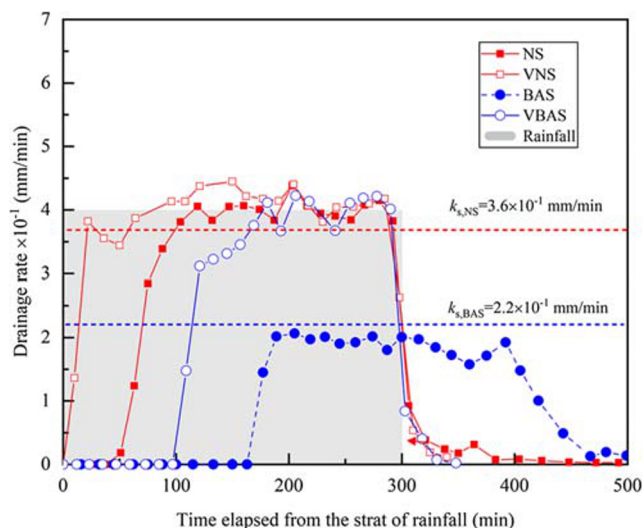

Fig. 5 Drainage rate of soil columns

Table 3 Estimated values of the van Genuchten hydraulic parameters obtained by inverse solution in HYDRUS-1D

Parameters	Units	Estimated values			
		NS	VNS	BAS	VBAS
θ_s	cm³/cm³	0.51	0.55	0.66	0.69
α	× 10⁻² cm⁻¹	3.01	1.96	0.51	0.43
n	-	1.30	1.25	1.23	1.20
k_s	× 10⁻² cm/min	3.56†	500.0	2.18†	16.1
R^2	-	0.99963	0.99961	0.99481	0.99919
RMSE	-	0.77e-1	0.86e-1	0.24e-1	0.90e-1

† Measured values

than those of natural soil columns (NS and VNS). It can be found a 15% increase of the saturated water content from VBAS to VNS and a 16% increase from BAS to NS. These results have a similar trend as some previous experimental reports [43, 44], even though the results obtained in this study are slightly higher than Garg et al. [43] (i.e., 13%) and Ni et al. [44] (i.e., 5%). The embedded effect caused by the particle size distribution of clay [45] and the different types of biochar may probably be responsible for the higher saturated water content. On the other hand, the saturated water content of vegetated soil columns was higher than the bare soil columns, with a 4% increase from VNS to NS and a 3% increase from VBAS to BAS. Leung et al. [46] reported a similar amount of increase in saturated water content (i.e., 4.5%), and pointed out that the plant roots could change the soil structure and thus affect the soil-water retention chrematistics.

Comparison between the vegetated soils and bare soils implied that the permeability of vegetated soil has increased in both columns with and without biochar mixture. As discussed in previous studies [26, 47], the preferential water flow channel formed by the growth of plant roots might contribute to the change of saturated hydraulic conductivity. Besides, the development of cracks during the daily irrigation process in vegetated soil may have a significant influence on the hydraulic conductivity [48].

It can be found that the biochar-amended soils have lower saturated hydraulic conductivity. One of the possible reasons is the higher degree of compaction (DOC) in biochar-amended soil samples (i.e., 75% for BAS and 67% for NS). The higher DOC might result in less volume of inter-pores among the clay aggregates. Meanwhile, biochar particles acted as a filling material among the clay particles and subsequently impeded the flow of water [49].

In conclusion, the vegetated soils have higher saturated hydraulic conductivity values and higher saturated water content, while the addition of biochar decreased the saturated hydraulic conductivity and increased the saturated water content of the soil. The combination of vegetation and biochar

(i.e., VBAS) shows the highest saturated water content among the four tested soil columns. The saturated hydraulic conductivity of VBAS was higher than NS and BAS but lower than that of VNS. This might be a comprehensive result of biochar and vegetation, which influenced by the growth condition of plant and biochar type. Considering that biochar may have benefits in plant growth, further studies are needed to understand the coupling effect of biochar and vegetation on the long-term hydraulic properties.

3.3 Stormwater management in biochar-amended substrate

To understand the rainstorm management of biochar-amended substrate, a set of measured rainstorm data was input in the HYDRUS-1D for simulation. The selected rainfall happened on May 22, 2020, and the rainfall data was recorded by a meteorological station on the campus of Guangxi University. The rain lasted for 10 h, with a maximum instantaneous rainfall intensity of 0.21 cm/min. The cumulative precipitation was up to 100 mm. The recorded rainfall data was set as the time-variable boundary conditions in the upper surface of the simulated model. The lower boundary condition was set as free drainage, which was able to reproduce the drainage condition of green roof substrates. For comparative purpose, all soil columns were set at the same initial water content (i.e., 0.3 m^3/m^3). The hydraulic parameters obtained from the inverse solution were input in the simulation (refer to Table 2). With these initial and boundary conditions, six types of green roof substrates were simulated, as shown in Table 4. The stormwater management (e.g., peak flow delay and reduction effect) of green roofs was compared and discussed between different biochar addition modes. These biochar addition modes can be classified as (1) single-layer mode with and without biochar-amended soil (substrate A and B), (2) two types of dual-layer modes: biochar mixed in the upper layer (substrate F), and biochar mixed in the bottom layer (substrate C, D, and E).

Figure 6a–f shows the flux of surface runoff and drainage during the rainstorm. The positive value represents the surface runoff, and the negative value denotes the bottom drainage. It can be found that there was no surface runoff from substrate A during the rainfall, and the other substrates generated both surface runoff and bottom drainage. During the light rain (0–100 min), there was no rainwater outflowed from each of the tested substrates. This is because of the sufficient storage capacity in the substrate before saturation, and the infiltration rate of the substrate was higher than the rain intensity. Along with an increase in rainfall intensity (100–145 min), the outflow from substrate A generated the earliest in the 116 min after rain beginning, and the substrate B showed the longest delay (i.e., 142 min) in the occurrence of rainwater outflow (refer to Table 5). For substrate A, no surface runoff was generated during the rain, and the outflow only came from the bottom drainage because of the higher saturated hydraulic conductivity than the rain intensity, while the substrate B generated a small quantity of surface runoff because its saturated hydraulic conductivity (i.e., 0.16 cm/min) was slightly lower than the maximum rainfall intensity (i.e., 0.21 cm/min). All the dual-layer substrates (i.e., substrate C, D, E, and F) generated both surface runoff and bottom drainage, and generally, the runoff occurred earlier than bottom drainage.

The rainstorm reached the maximum intensity of 0.21 cm/min at the 145 min, followed by the peak outflow from each substrate. As shown in Table 5, substrate F showed a longest peak-outflow delay (i.e., 6 min), and then substrate A, B, and C, while substrate E shows no peak-outflow delay. As shown in Fig. 7, the rainwater divided into three parts in most substrates (i.e., runoff, storage, and drainage) according to the flow direction. The occurrence of surface runoff and bottom drainage depended on the infiltration rate and storage capacity of the substrates. This might result in different delay effect and reduction in peak outflow. Among the tested substrates, substrate C showed the highest reduction in peak outflow, followed by substrate F, while substrate D and substrate E show no reduction. This was mainly due to the off-peak effect in the occurrence of runoff and drainage in these two substrates.

Table 4 Outflow reduction and delay effect of different substrates

Substrates	Substrate layers			
	Material of upper layer	Height of upper layer	Material of lower layer	Material of lower layer
A	VNS			
B	VBAS			
C	VNS	3 cm	BAS	12 cm
D	VNS	7.5 cm	BAS	7.5 cm
E	VNS	12 cm	BAS	3 cm
F	VBAS	7.5 cm	NS	7.5 cm

Table 5 Outflow reduction and delay effect of different substrates

Substrates	Reduction of peak outflow × 10⁻¹ (cm/min)	Peak outflow delay (min)	Rainwater outflow delay (min)
A	0.06	5	116
B	0.24	5	142
C	0.57	5	122
D	0	3	131
E	0	0	130
F	0.35	6	127

Even though the surface runoff came out earlier in these two substrates, the runoff flux reduced the infiltration flux and assumed the distributary role. Therefore, the occurrence of bottom drainage was further delay. In addition, the higher storage volume of substrate C in comparison to other substrates (refer to Fig. 7) suggests a higher detention capacity and provides a better delay and reduction effect, whereas substrate D and E had generated the runoff and drainage before the maximum rainfall intensity, which indicated that the substrate has reached saturation. The precipitation divided into two parts (i.e., runoff and drainage) after the substrate reached its storage capacity; thus, the peak flow delay and reduction effect have been decreased.

3.4 Prospect of the biochar-amended green roofs

The benefits of biochar as a soil amendment in green roofs have been investigated extensively. Studies indicated that different application modes have resulted in varying runoff quality, quantity [50], and nitrogen dynamics, which is important

for plant growth [8]. Compared to the situation in slope and landfill cover, it is much more convenient to mix biochar particles in layers for the construction of green roof. In present study, a new biochar application mode with dual-layer substrate was proposed. Substrates with similar structure have been proved to be effective in retaining rainfall and pollution reduction [51]. Simulation results show that different substrate structures (i.e., upper layer with natural soil and bottom layer with biochar-amended soil) and the height of biochar-amended layer can cause different peak flow delay and reduction effects in green roofs. An optimum structure of biochar-amended substrate can be designed based on the local climate conditions. However, the following factors should be considered before using biochar in substrate:

3.4.1 Pyrolysis effect

Feedstock type and pyrolysis temperature may significantly change the physio-chemical characteristics of biochar. Studies showed that the treatment process of biochar can influence the
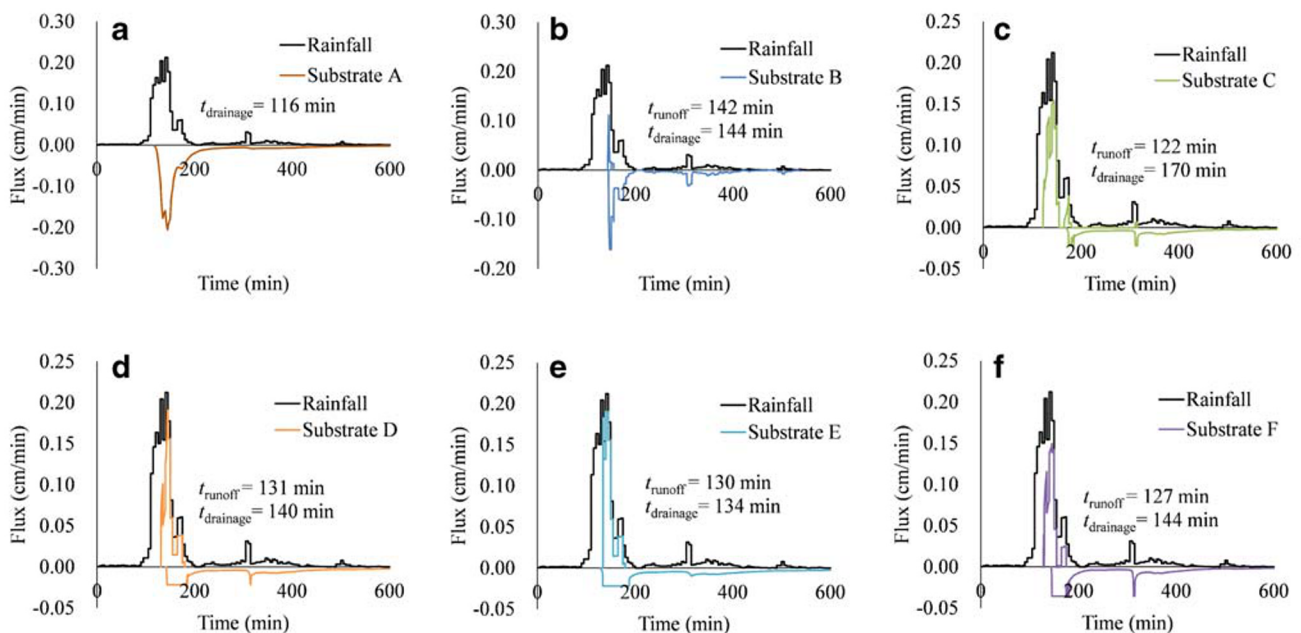
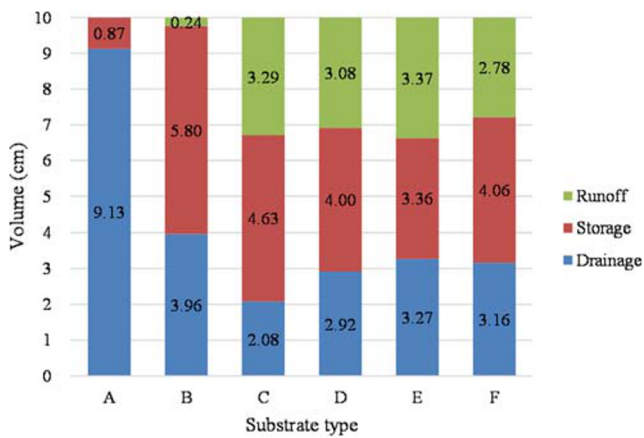**Fig. 6** The flux of surface runoff and bottom drainage from different substrates

Fig. 7 The volume of rainwater outflow

pyrogenic nano-pores and hydrophobic surfaces [52], and therefore affect the hydraulic properties such as soil water retention and plant available water [53, 54]. It was suggested that higher pyrolysis temperature is likely to lead to higher hydrophobicity of biochar. Furthermore, volatilization of organic compounds in the feedstock under higher pyrolysis temperature would enhance surface area and pores formation [55]. Apart from this, application rate, soil type, and particle size of biochar may also influence hydraulic properties of biochar amended soil [56]. The hydraulic performance of biochar-amended substrate can only be determined after obtaining the hydraulic parameters of the specific biochar type and soil mixture.

3.4.2 Biochar aging

The aging or weathering of biochar with time in a field is likely to cause changes in physiochemical properties and disintegration of biochar into smaller particles [57]. The change in porosity due to aging alters the soil water retention characteristics (SWRC). Paetsch et al. [58] found a higher water retention in a 3-year-aged biochar-amended soil compared to the soil with fresh biochar from same feedstock and pyrolysis process. Aller et al. [11] found that the effect of aged and fresh biochar on water retention varied with the soil type, and pointed out that aged biochar is more hydrophilic then fresh biochar. Based on literatures, the influence of fresh and aged biochar on soil hydraulic properties is highly variable, which may depend on biochar type and soil type.

3.4.3 Cost-benefit analysis

Unlike other natural material commonly used for green roofs (e.g., coir, peat, sewage sludge, and farmyard waste), biochar is a stable, carbon-rich charcoal that results from pyrolysis of biomass materials, accompany with gas and oils [59]. The manufacturing process of biochar provided some additional benefits such as potential for C sequestration, reductions in

greenhouse gas emission, renewable energy generation, and economic viability [60]. The feedstock collection and pyrolysis process are the main cost of the biochar application in green roofs. Waste biomass such as water hyacinth may have the greatest potential to be economically viable while still being net energy positive [17].

In conclusion, we suggested that the feedstock collection should be obtained from the local waste material (i.e., near testing site) to minimize the cost of biochar production, transportation, and site application. Systematic studies including effects of feedstock selection, pyrolysis effect, biochar aging, nutrient leaching, and the biochar application mode (i.e., layer height of biochar-amended substrate) on water dynamics under local climate conditions are needed for preliminary design of biochar-amended green roofs.

4 Conclusion

This study aims to evaluate the hydraulic performance of green roofs with biochar and optimize its ability in stormwater management. To achieve these goals, four experimental soil columns were built to observe the hydraulic processes under artificial rainfall. Unsaturated hydraulic parameters of soils were derived in four column tests using inverse analysis. Numerical simulations were conducted to explore the mechanism of stormwater management performance in dual-layer biochar-amended substrates. Following can be concluded from study:

> Unsaturated hydraulic parameters were derived for four experimental columns using inverse analysis. The simulation results show high agreement with the measured results. The derived parameters were able to reflect the hydraulic characteristics and the models were able to capture the surface runoff and bottom drainage of these substrate materials.
> The vegetated soil has higher saturated water content and saturated hydraulic conductivity, whereas biochar-amended soil has higher saturated water content but shows a lower permeability than natural soil. The vegetated biochar-amended soil (VBAS) has the highest saturated water content among the four tested substrate materials, but the saturated hydraulic conductivity of VBAS was lower than vegetated natural soil.
> For utilizing higher water retention capacity of biochar-amended soil and permeability of natural soil, dual-layer biochar-amended substrate is proposed for green roofs. The different height ratio of the layers showed variation in peak-outflow delay and reduction. The case study simulated under measured rainfall data showed that under the given substrate thickness (i.e., 15 cm), dual-layer substrate with 3 cm vegetated natural soil in the upper layer

and 12 cm biochar-amended soil possessed a longer delay and higher reduction in peak outflow and thus provide the highest rainwater storage capacity.

Besides the hydraulic performance, the economic viability and environmental sustainability should be taken into consideration. Comprehensive studies including feedstock selection, pyrolysis effect, biochar aging, nutrient leaching, and the biochar application mode based on the local climate are needed before the biochar used in the green roofs substrate.

The dual-layer substrate with biochar-amended soil is a flexible utilization of biochar in green roofs. Biochar, being a more stable material (expected half-life greater than 100 years [10]), is more feasible amendment than other types of biomass (coir, peat, sewage sludge and farmyard waste, etc.). This study also can help in preliminary design of green roof by considering native vegetation, local soil, and climatic conditions. Further studies are needed to combine the probabilistic analysis and provide a design guideline for optimizing the rainstorm management of green roofs.

Data availability The data that support the findings of this study are available from the corresponding.

Compliance with ethical standards

Conflict of interest The authors declare that they have no conflict of interest.

Code availability The software HYDRUS-1D (ver. 4.16) was provided by a third party (PC-Progress s.r.o.). This software is an open source code which it is available online (www.pc-progress.com).

References

1. Jha RK, Sahoo B, Panda RK (2017) Modeling the water and nitrogen transports in a soil–paddy–atmosphere system using HYDRUS-1D and lysimeter experiment. Paddy Water Environ 15:831–846. https://doi.org/10.1007/s10333-017-0596-9

2. Zheng C, Lu Y, Guo X et al (2017) Application of HYDRUS-1D model for research on irrigation infiltration characteristics in arid oasis of northwest China. Environ Earth Sci 76:785. https://doi.org/10.1007/s12665-017-7151-2

3. Jin C, Bai X, Luo T, Zou M (2018) Effects of green roofs' variations on the regional thermal environment using measurements and simulations in Chongqing, China. Urban For Urban Green 29:223–237. https://doi.org/10.1016/j.ufug.2017.12.002

4. Yang W-Y, Li D, Sun T, Ni G-H (2015) Saturation-excess and infiltration-excess runoff on green roofs. Ecol Eng 74:327–336. https://doi.org/10.1016/j.ecoleng.2014.10.023

5. Rasa K, Heikkinen J, Hannula M, Arstila K, Kulju S, Hyväluoma J (2018) How and why does willow biochar increase a clay soil water retention capacity? Biomass Bioenergy 119:346–353. https://doi.org/10.1016/j.biombioe.2018.10.004

6. Cao CTN, Farrell C, Kristiansen PE, Rayner JP (2014) Biochar makes green roof substrates lighter and improves water supply to plants. Ecol Eng 71:368–374. https://doi.org/10.1016/j.ecoleng.2014.06.017

7. Kuoppamäki K, Lehvävirta S (2016) Mitigating nutrient leaching from green roofs with biochar. Landsc Urban Plan 152:39–48. https://doi.org/10.1016/j.landurbplan.2016.04.006

8. Lu H, Feng Y, Gao Q, Xing J, Chen Y, Yang L, Xue L (2020) Surface soil mixing is more beneficial than the plough layer mixing mode of biochar application for nitrogen retention in a paddy system. Sci Total Environ 718:137399. https://doi.org/10.1016/j.scitotenv.2020.137399

9. Ladygina N, Rineau F (2013) Biochar ands oil biota. CRC Press, New York, USA

10. Lehmann J (2007) Bio-energy in the black. Front Ecol Environ 5(7):381–387. https://doi.org/10.1890/1540-9295(2007)5[381:Bitb]2.0.Co;2

11. Aller D, Rathke S, Laird D, Cruse R, Hatfield J (2017) Impacts of fresh and aged biochars on plant available water and water use efficiency. Geoderma 307:114–121. https://doi.org/10.1016/j.geoderma.2017.08.007

12. Günal E, Erdem H, Çelik İ (2018) Effects of three different biochars amendment on water retention of silty loam and loamy soils. Agric Water Manag 208:232–244. https://doi.org/10.1016/j.agwat.2018.06.004

13. Huang ZQ, Hu LC, Zhou Q, Guo Y, Tang W, Dai JY (2018) Effect of aging on surface chemistry of rice husk-derived biochar. Environ Prog Sustain 37(1):410–417. https://doi.org/10.1002/ep.12694

14. Abrol V, Ben-Hur M, Verheijen FGA, Keizer JJ, Martins MAS, Tenaw H, Tchehansky L, Graber ER (2016) Biochar effects on soil water infiltration and erosion under seal formation conditions: rainfall simulation experiment. J Soils Sediments 16(12):2709–2719. https://doi.org/10.1007/s11368-016-1448-8

15. Lim TJ, Spokas KA, Feyereisen G, Novak JM (2016) Predicting the impact of biochar additions on soil hydraulic properties. Chemosphere 142:136–144. https://doi.org/10.1016/j.chemosphere.2015.06.069

16. Mohawesh O, Durner W (2019) Effects of bentonite, hydrogel and biochar amendments on soil hydraulic properties from saturation to oven dryness. Pedosphere 29(5):598–607. https://doi.org/10.1016/s1002-0160(17)60426-0

17. Bordoloi S, Garg A, Sreedeep S, Lin P, Mei G (2018) Investigation of cracking and water availability of soil-biochar composite synthesized from invasive weed water hyacinth. Bioresour Technol 263:665–677. https://doi.org/10.1016/j.biortech.2018.05.011

18. Gopal P, Bordoloi S, Ratnam R, Lin P, Cai W, Buragohain P, Garg A, Sreedeep S (2019) Investigation of infiltration rate for soil-biochar composites of water hyacinth. Acta Geophys 67(1):231–246. https://doi.org/10.1007/s11600-018-0237-8

19. Berretta C, Poë S, Stovin V (2014) Reprint of "moisture content behaviour in extensive green roofs during dry periods: the influence of vegetation and substrate characteristics". J Hydrol 516:37–49. https://doi.org/10.1016/j.jhydrol.2014.04.001

20. Beck DA, Johnson GR, Spolek GA (2011) Amending greenroof soil with biochar to affect runoff water quantity and quality. Environ Pollut 159(8-9):2111–2118. https://doi.org/10.1016/j.envpol.2011.01.022

21. Chen H, Ma J, Wei J, Gong X, Yu X, Guo H, Zhao Y (2018) Biochar increases plant growth and alters microbial communities via regulating the moisture and temperature of green roof substrates. Sci Total Environ 635:333–342. https://doi.org/10.1016/j.scitotenv.2018.04.127

22. Olszewski MW, Eisenman SW (2017) Influence of biochar amendment on herb growth in a green roof substrate. Hortic Environ Biotechnol 58(4):406–413. https://doi.org/10.1007/s13580-017-0180-7

23. Pant A, Ramana GV, Datta M, Gupta SK (2019) Coal combustion residue as structural fill material for reinforced soil structures. J Clean Prod 232:417–426. https://doi.org/10.1016/j.jclepro.2019.05.354

24. Emilsson T, Rolf K (2005) Comparison of establishment methods for extensive green roofs in southern Sweden. Urban For Urban Green 3(2):103–111. https://doi.org/10.1016/j.ufug.2004.07.001

25. Dresbøll DB (2010) Effect of growing media composition, compaction and periods of anoxia on the quality and keeping quality of potted roses (Rosa sp.). Sci Hortic 126(1):56–63. https://doi.org/10.1016/j.scienta.2010.06.004

26. Li JH, Li L, Chen R, Li DQ (2016) Cracking and vertical preferential flow through landfill clay liners. Eng Geol 206:33–41. https://doi.org/10.1016/j.enggeo.2016.03.006

27. Zhang J, Poudel B, Kenworthy K, Unruh JB, Rowland D, Erickson JE, Kruse J (2019) Drought responses of above-ground and below-ground characteristics in warm-season turfgrass. J Agron Crop Sci 205(1):1–12. https://doi.org/10.1111/jac.12301

28. Anangsha A, Gadi VK, Bordoloi S, Kothapalli SK, Sreedeep S, Guoxiong M, Garg A (2019) A new autonomous program customized for computing surface cracks in an unsaturated soil in a 1-D column. J Test Eval 47(5):3822–3835. https://doi.org/10.1520/jte20180609

29. Quinn R, Dussaillant A (2018) The impact of macropores on heavy metal retention in sustainable drainage systems. Hydrol Res 49(2):517–527. https://doi.org/10.2166/nh.2018.277

30. Berghage RD, Beattie D, Jarrett AR (2009) Green roofs for stormwater runoff countrol. United States Environmental Protectio Agency, United States

31. Di Prima S, Castellini M, Abou Najm MR, Stewart RD, Angulo-Jaramillo R, Winiarski T, Lassabatere L (2019) Experimental assessment of a new comprehensive model for single ring infiltration data. J Hydrol 573:937–951. https://doi.org/10.1016/j.jhydrol.2019.03.077

32. Liu R, Fassman-Beck E (2017) Hydrologic response of engineered media in living roofs and bioretention to large rainfalls: experiments and modeling. Hydrol Process 31(3):556–572. https://doi.org/10.1002/hyp.11044

33. Ministry of Housing and Urban-Rural Development of the People's of Republic of China (MOHURD) (2014) Code for design of outdoor wastewater engineering 2014 Edition (GB50014-2006). China Planning Press, China

34. Shao D, Liu G-S (2018) Up-to-date urban rainstorm intensity formulas considering spatial diversity in China. Environ Earth Sci 77(14):1–12. https://doi.org/10.1007/s12665-018-7718-6

35. Liu BH, Xu M, Henderson M, Gong WG (2004) A spatial analysis of pan evaporation trends in China, 1955–2000. J Geophys Res 109(D15):D15102. https://doi.org/10.1029/2004jd004511

36. Ni JJ, Bordoloi S, Shao W, Garg A, Xu G, Sarmah AK (2020) Two-year evaluation of hydraulic properties of biochar-amended vegetated soil for application in landfill cover system. Sci Total Environ 712:136486. https://doi.org/10.1016/j.scitotenv.2019.136486

37. Leung AK, Garg A, Coo JL, Ng CWW, Hau BCH (2015) Effects of the roots of Cynodon dactylon and Schefflera heptaphylla on water infiltration rate and soil hydraulic conductivity. Hydrol Process 29(15):3342–3354. https://doi.org/10.1002/hyp.10452

38. Šimůnek J, Šejna M, Saito H, Sakai M, van Genuchten MT (2008) The HYDRUS-1D software package for simulating the movement of water, heat, and multiple solutes in variably saturated media Version 4.0, HYDRUS Software Series 3. Department of Environmental Sciences, University of California Riverside, Riverside, California, USA

39. Hilten RN, Lawrence TM, Tollner EW (2008) Modeling stormwater runoff from green roofs with HYDRUS-1D. J Hydrol 358(3-4):288–293. https://doi.org/10.1016/j.jhydrol.2008.06.010

40. Marquardt DW (1963) An algorithm for least-squares estimation of nonlinear parameters. J Soc Ind Appl Math 11(2):431–441. https://doi.org/10.1137/0111030

41. Kelleners TJ, Soppe RWO, Ayars JE, Šimůnek J, Skaggs TH (2005) Inverse analysis of upward water flow in a groundwater table lysimeter. Vadose Zone J 4(3):558–572. https://doi.org/10.2136/vzj2004.0118

42. Mualem Y (1976) A new model for predicting the hydraulic conductivity of unsaturated porous media. Water Resour Res 12(3):513–522. https://doi.org/10.1029/WR012i003p00513

43. Garg A, Bordoloi S, Ni J, Cai W, Maddibiona PG, Mei G, Poulsen TG, Lin P (2019) Influence of biochar addition on gas permeability in unsaturated soil. Géotech Lett 9(1):66–71. https://doi.org/10.1680/jgele.18.00190

44. Ni JJ, Chen XW, Ng CWW, Guo HW (2018) Effects of biochar on water retention and matric suction of vegetated soil. Géotech Lett 8(2):124–129. https://doi.org/10.1680/jgele.17.00180

45. Wong JTF, Chen Z, Chen X, Ng CWW, Wong MH (2016) Soil-water retention behavior of compacted biochar-amended clay: a novel landfill final cover material. J Soils Sediments 17(3):590–598. https://doi.org/10.1007/s11368-016-1401-x

46. Leung AK, Garg A, Ng CWW (2015) Effects of plant roots on soil-water retention and induced suction in vegetated soil. Eng Geol 193:183–197. https://doi.org/10.1016/j.enggeo.2015.04.017

47. Devitt DA, Smith SD (2002) Root channel macropores enhance downward movement of water in a Mojave Desert ecosystem. J Arid Environ 50(1):99–108. https://doi.org/10.1006/jare.2001.0853

48. Rayhani MH, Yanful EK, Fakher A (2007) Desiccation-induced cracking and its effect on the hydraulic conductivity of clayey soils from Iran. Can Geotech J 44(3):276–283. https://doi.org/10.1139/t06-125

49. Wong JTF, Chen Z, Ng CWW, Wong MH (2016) Gas permeability of biochar-amended clay: potential alternative landfill final cover material. Environ Sci Pollut Res 23(8):7126–7131. https://doi.org/10.1007/s11356-015-4871-2

50. Kuoppamäki K, Hagner M, Lehvävirta S, Setälä H (2016) Biochar amendment in the green roof substrate affects runoff quality and quantity. Ecol Eng 88:1–9. https://doi.org/10.1016/j.ecoleng.2015.12.010

51. Wang X, Tian Y, Zhao X (2017) The influence of dual-substrate-layer extensive green roofs on rainwater runoff quantity and quality. Sci Total Environ 592:465–476. https://doi.org/10.1016/j.scitotenv.2017.03.124

52. Gray M, Johnson MG, Dragila MI, Kleber M (2014) Water uptake in biochars: the roles of porosity and hydrophobicity. Biomass Bioenergy 61:196–205. https://doi.org/10.1016/j.biombioe.2013.12.010

53. Marshall J, Muhlack R, Morton BJ, Dunnigan L, Chittleborough D, Kwong CW (2019) Pyrolysis temperature effects on biochar–water interactions and application for improved water holding capacity in vineyard soils. Soil Syst 3(2):27. https://doi.org/10.3390/soilsystems3020027

54. Mollinedo J, Schumacher TE, Chintala R (2015) Influence of feedstocks and pyrolysis on biochar's capacity to modify soil water retention characteristics. J Anal Appl Pyrolysis 114:100–108. https://doi.org/10.1016/j.jaap.2015.05.006

55. Jeong CY, Dodla SK, Wang JJ (2016) Fundamental and molecular composition characteristics of biochars produced from sugarcane and rice crop residues and by-products. Chemosphere 142:4–13. https://doi.org/10.1016/j.chemosphere.2015.05.084

56. Wiersma W, van der Ploeg MJ, Sauren IJMH, Stoof CR (2020) No effect of pyrolysis temperature and feedstock type on hydraulic properties of biochar and amended sandy soil. Geoderma 364: 114209. https://doi.org/10.1016/j.geoderma.2020.114209

57. Hussain R, Garg A, Ravi K (2020) Soil-biochar-plant interaction: differences from the perspective of engineered and agricultural soils. Bull Eng Geol Environ 79:4461–4481. https://doi.org/10.1007/s10064-020-01846-3

58. Paetsch L, Mueller CW, Kogel-Knabner I, von Lutzow M, Girardin C, Rumpel C (2018) Effect of in-situ aged and fresh biochar on soil hydraulic conditions and microbial C use under drought conditions. Sci Rep 8(1):6852. https://doi.org/10.1038/s41598-018-25039-x

59. Abhijeet P, Swagathnath G, Rangabhashiyam S, Asok Rajkumar M, Balasubramanian P (2019) Prediction of pyrolytic product composition and yield for various grass biomass feedstocks. Biomass Convers Bioref 10(3):663–674. https://doi.org/10.1007/s13399-019-00475-5

60. Roberts KG, Gloy BA, Joseph S, Scott NR, Lehmann J (2010) Life cycle assessment of biochar systems: estimating the energetic, economic, and climate change potential. Environ Sci Technol 44(2): 827–833. https://doi.org/10.1021/es902266r

Publisher's Note Springer Nature remains neutral with regard to jurisdictional claims in published maps and institutional affiliations.